Available online at www.sciencedirect.com
SCIENCE DIRECT®
Catalysis Today 100 (2005) 37–47
CATALYSIS TODAY
www.elsevier.com/locate/cattod

# Selective catalytic reduction of $NO_x$ over $Ag/Al_2O_3$ catalyst: from reaction mechanism to diesel engine test

Hong He *, Yunbo Yu

*Research Center for Eco-Environmental Sciences, Chinese Academy of Sciences, Beijing 100085, P.R. China*

Available online 24 March 2005

**Abstract**

Our recent research works on the selective catalytic reduction (SCR) of diesel engine $NO_x$ by hydrocarbons over alumina-supported silver ($Ag/Al_2O_3$) were reviewed. The reaction mechanism of the SCR of $NO_x$ by $C_2H_5OH$ over $Ag/Al_2O_3$ was studied using in situ DRIFTS and DFT calculations. A novel enolic species originating from the partial oxidation of $C_2H_5OH$ and $C_3H_6$, was found on the surface of $Ag/Al_2O_3$ during the SCR of $NO_x$ by in situ DRIFTS, which was also supported by DFT calculations. Based on this, a mechanism of the $NO_x$ reduction was proposed, which can successfully explain the high efficiency of the $NO_x$ reduction by $C_2H_5OH$ over $Ag/Al_2O_3$. A palladium promoted $Ag/Al_2O_3$ catalyst (denoted $Ag–Pd/Al_2O_3$) was developed for the SCR of $NO_x$ by $C_3H_6$. The $Ag–Pd/Al_2O_3$ showed a higher $NO_x$ conversion than $Ag/Al_2O_3$, especially at temperatures ranging from 300 to 450 °C. The engine bench tests showed that the average $NO_x$ conversion was greater than 80% in the diesel engine exhaust temperature range of 300–400 °C using our catalytic converter with $C_2H_5OH$ as reductant, which represents a leap from the Euro II standard to the Euro III standard for $NO_x$ emission control in diesel engines.


*Keywords:* Selective catalytic reduction (SCR) of $NO_x$; Alumina supported silver ($Ag/Al_2O_3$); Ethanol ($C_2H_5OH$); Diesel engine; Enolic species

## 1. Introduction

Due to shortages of petroleum resources, lean-burn engines have become the main option for the vehicles. The diesel engine, which is a typical lean-burn engine, has the advantage of lower consumption of fuel and lower emission of $CO_2$, CO and HC than stoichiometric gasoline engine. However, the exhaust from diesel engines contains a large amount of $NO_x$ compared to stoichiometric gasoline engines equipped with three-way catalysts (TWCs). For a stoichiometric gasoline engine, a TWC provides a very high level of emission control for the removal of CO, $NO_x$, and unburnt hydrocarbons. However, diesel engines produce exhaust containing a large excess of oxygen. The platinum group metals based TWCs are completely ineffective for $NO_x$ reduction under the oxygen-rich conditions. Removal of $NO_x$ in the oxygen-rich exhausts demands a novel catalyst for a selective catalytic reduction (SCR) of $NO_x$. The SCR of $NO_x$ by ammonia, or in some cases, urea, has become a fairly mature technology for stationary applications [1–4]. For mobile applications such as diesel trucks and some lean-burn gasoline cars, however, commercialization still lies somewhere in the future. Up to now, multifarious catalysts such as zeolitic oxide, base oxide/metal and noble metal catalysts have been found to be effective for $NO_x$ reduction in the presence of excess oxygen [3,5–8]. Among them $Ag/Al_2O_3$ is known as one of the most effective catalysts for the SCR of $NO_x$ by hydrocarbons [9–45]. In particular, $C_2H_5OH$ is extremely effective for $NO_x$ reduction over $Ag/Al_2O_3$ [10,11,17,36,38,41,46–51].

In this review, our recent research on the HC–SCR of $NO_x$ over $Ag/Al_2O_3$ was summarized systematically on a laboratory scale and an actual diesel engine bench scale. Also, our results provided new insight into the mechanism of this $NO_x$ reduction process.

## 2. Characterization and fundamental performance of $Ag/Al_2O_3$ in the SCR of $NO_x$

The supported catalysts, $Ag/Al_2O_3$ and $Cu/Al_2O_3$, were prepared by an impregnation method with an aqueous solution of silver and copper nitrate, followed by evapora-

* Corresponding author. Tel.: +86 10 62849123; fax: +86 10 62849123.
*E-mail address:* honghe@mail.rcees.ac.cn (H. He).

0920-5861/$ – see front matter © 2004 Elsevier B.V. All rights reserved.
doi:10.1016/j.cattod.2004.11.006

Table 1
BET surface area, pore volume and pore diameter of $Ag/Al_2O_3$ catalysts with different Ag loadings

| Catalyst | BET surface area ($m^2\ g^{-1}$) | Pore volume ($cc\ g^{-1}$) | Pore diameter (A) |
|---|---|---|---|
| 2 wt.% $Ag/Al_2O_3$ | 239.8 | 0.7235 | 122.9 |
| 4 wt.% $Ag/Al_2O_3$ | 222.4 | 0.7107 | 124.9 |
| 6 wt.% $Ag/Al_2O_3$ | 211.8 | 0.6950 | 126.2 |
| 8 wt.% $Ag/Al_2O_3$ | 209.9 | 0.6493 | 130.3 |

tion to dryness in a rotary evaporator under pressure reduction at 60 °C. The wet sample was dried at 120 °C for 12 h, and then calcined in air at 600 °C for 3 h [39].

BET results of the catalysts are shown in Table 1. The surface area of the $Ag/Al_2O_3$ catalysts gradually decreased with increasing silver loading. XRD patterns of a series of $Ag/Al_2O_3$ catalysts are shown in Fig. 1. Only the $\gamma$-$Al_2O_3$ phase was detected as the silver loading increased from 2 to 6 wt.%, but the Ag and $Ag_2O$ phases were observed at $2\theta$ of 33.76°, 38.12°, 44.36° and 64.46° with 8 wt.% Ag loading [52,53]. TEM images of 4% $Ag/Al_2O_3$ catalyst are shown in Fig. 2. The Ag containing particles could be distributed evenly on the surface of $Al_2O_3$ with an optimum Ag loading of 4–6% and an average size of 15 nm.

Fig. 3 shows the $NO_x$ conversions for the SCR of $NO_x$ by $C_3H_6$ over $Ag/Al_2O_3$ catalysts with different silver loadings at various temperatures. The maximum of $NO_x$ conversion increased significantly with an increase in silver loading from 2 to 4 wt.%, and the temperature at which the maximum $NO_x$ conversion could be obtained (i.e. $T_{max}$) shifted towards a lower temperature. Further increase of the silver loading from 4 to 8 wt.% did not show any promotion of low-temperature $NO_x$ conversion but inhibited the high temperature conversion.

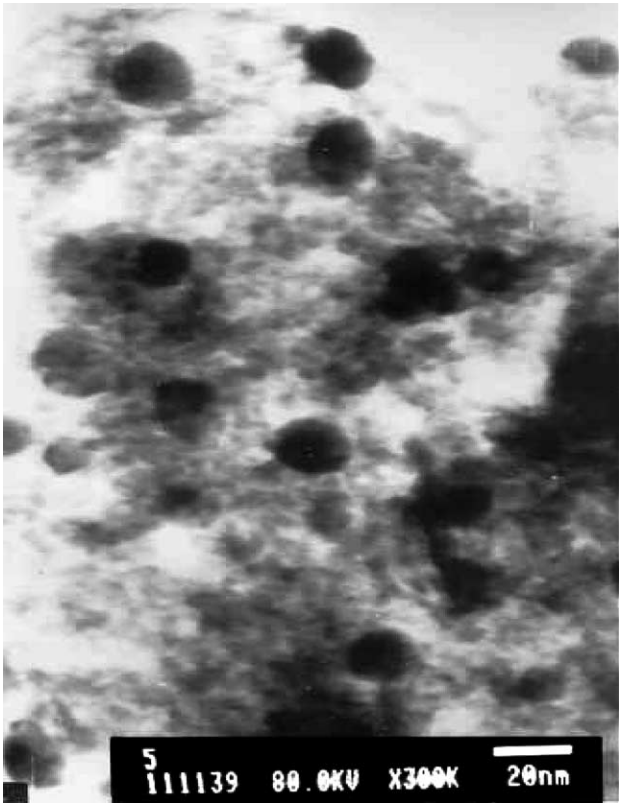


Fig. 2. TEM image of 4% $Ag/Al_2O_3$.

The $NO_x$ conversions for the SCR of $NO_x$ by $C_2H_5OH$ over $Ag/Al_2O_3$ catalysts with different silver loadings are shown in Fig. 4. As same as in Fig. 3, the maximum of $NO_x$ conversion increased significantly with an increase in silver loading from 2 to 4 wt.%, and the temperature at which the

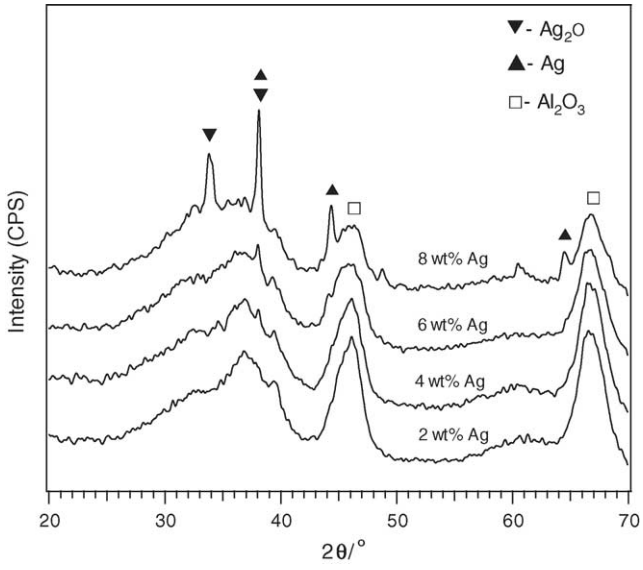


Fig. 1. XRD patterns of $Ag/Al_2O_3$ catalysts with different Ag loadings [39].

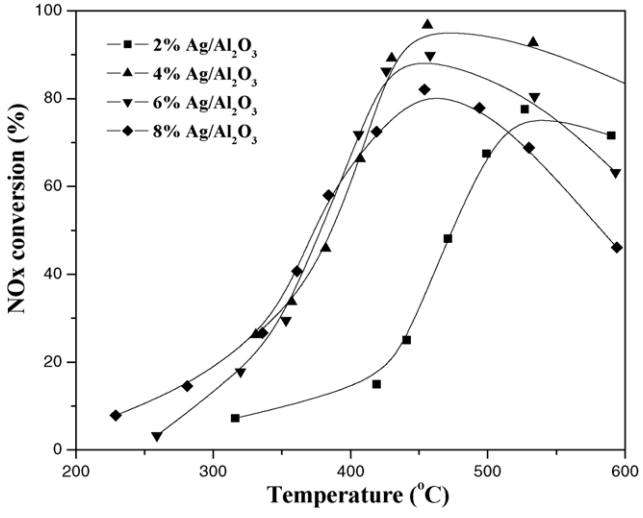


Fig. 3. $NO_x$ conversion for the SCR of $NO_x$ by $C_3H_6$ over $Ag/Al_2O_3$: (■) 2 wt.%, (▲) 4 wt.%, (▼) 6 wt.% and (◆) 8 wt.% at various temperatures. Conditions: 800 ppm NO, 1714 ppm $C_3H_6$, 10 vol.% $O_2/N_2$, catalyst weight = 1.2 g, $W/F$ = 0.018 g s $cm^{-3}$ [39].

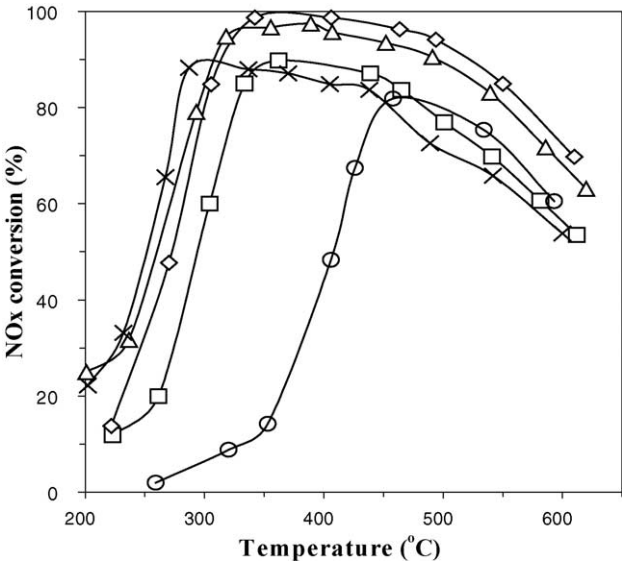


Fig. 4. NOx conversion over $Ag/Al_2O_3$ with different Ag loading: (□) 2 wt.% Ag and $C_2H_5OH$ as reductant, (◇) 4 wt.% Ag and $C_2H_5OH$ as reductant, (Δ) 6 wt.% Ag and $C_2H_5OH$ as reductant, (×) 8 wt.% Ag and $C_2H_5OH$ as reductant, and (○) 4 wt.% Ag and $C_3H_6$ as reductant. Conditions: 800 ppm NO, 1565 ppm $C_2H_5OH$, 10 vol.% $O_2/N_2$, 10 vol.% $H_2O$, catalyst weight = 1.2 g, $W/F = 0.018$ g s $cm^{-3}$.

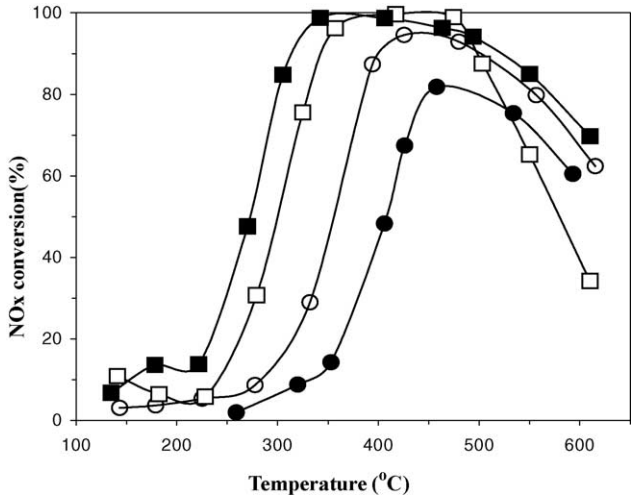


Fig. 5. Activity of $Ag/Al_2O_3$ for the SCR of $NO_x$ by: $C_3H_6$ (○), $C_3H_6 + H_2O$ (●), $C_2H_5OH$ (□), and $C_2H_5OH + H_2O$ (■). Conditions ($C_3H_6$): 800 ppm NO, 1714 ppm $C_3H_6$, 10 vol.% $O_2/N_2$, 0 or 10 vol.% $H_2O$, catalyst weight = 1.2 g, $W/F = 0.018$ g s $cm^{-3}$. Conditions ($C_2H_5OH$): 800 ppm NO, 1565 ppm $C_2H_5OH$, 10 vol.% $O_2/N_2$, 0 or 10 vol.% $H_2O$, catalyst weight = 1.2 g, $W/F = 0.018$ g s $cm^{-3}$.

maximum $NO_x$ conversion was obtained shifted towards a lower temperature. Further increase of the silver loading from 4 to 8 wt.% still enhanced the $NO_x$ conversion at low temperatures but decreased the $NO_x$ conversion at high temperatures. Since the 4 wt.% $Ag/Al_2O_3$ catalyst showed high activity for $NO_x$ reduction in both cases using $C_3H_6$ or $C_2H_5OH$ as a reductant, all of the $Ag/Al_2O_3$ catalysts that appeared below had a silver loading of 4 wt.%.

Fig. 5 shows a comparison of the performance of $Ag/Al_2O_3$ under different reaction conditions. When $C_3H_6$ was used as a reductant, the maximal conversion of $NO_x$ reached 94.5% in the absence of water vapor (○ curve). The addition of 10% water vapor to the gas stream resulted in a drastic decrease of the average $NO_x$ conversion, especially at the temperature range of 300–500 °C (● curve). However, the effect of water vapor was temporary and reversible. That is, when the addition of water vapor was stopped, the $NO_x$ conversion recovered to its initial level in the absence of water vapor, and $C_3H_6$ conversion and $CO_2$ formation also showed the same level of recovery (data not shown). A similar temporal effect of water vapor was also observed when other hydrocarbons were used as reductants. In the case of $C_2H_5OH$, however, the presence of water vapor did not decrease the $NO_x$ conversion, but enhanced the activity of $Ag/Al_2O_3$. In the diesel exhaust temperature region of 320–520 °C, the $NO_x$ reduction was greater than 90% (■ curve). It is worth noting that, even in the presence of $SO_2$, the $NO_x$ reduction by $C_2H_5OH$ over $Ag/Al_2O_3$ hardly changed, which provided an opportunity for practical usage in a $SO_2$ containing exhaust. On the basis of these results, we selected $Ag/Al_2O_3$–$C_2H_5OH$ as a promising combination of catalyst and reductant for $NO_x$ reduction in diesel engine exhaust.

## 3. Mechanism of the SCR of $NO_x$ by $C_2H_5OH$ over $Ag/Al_2O_3$

### 3.1. Formation of enolic species

Many researchers have intensively studied the reaction mechanism of the SCR of $NO_x$ [11,13,16–19,24–28,31–34,47–50]. Our earlier work was focused on the formation and reactivity of isocyanate (NCO) species on $Ag/Al_2O_3$ [16]. A possible mechanism for $NO_x$ reduction by $C_2H_5OH$ over $Ag/Al_2O_3$ was judged to be similar to that of $C_3H_6$: approximately, $NO + O_2 + C_2H_5OH \rightarrow NO_x$ (nitrate in particular) + $C_xH_yO_z$ (acetate in particular) → R–$NO_2$ + R–ONO → –NCO + –CN + NO + $O_2$ → $N_2$ [7,28]. However, this mechanism does not sufficiently explain why $C_2H_5OH$ has a higher efficiency for the SCR of $NO_x$ over $Ag/Al_2O_3$ than hydrocarbons such as $C_3H_6$.

In our recent papers [36–41], the formation and dynamic performance of partial oxidation products of $C_2H_5OH$ and $C_3H_6$ over $Ag/Al_2O_3$ were studied by an in situ diffuse reflectance infrared Fourier transform spectroscopy (DRIFTS) method, and we found a novel enolic species originating from the partial oxidation of $C_2H_5OH$. As shown in Fig. 6, peaks at 1579 and 1466 $cm^{-1}$ were due to acetate. Peaks at 1633, 1416 and 1336 $cm^{-1}$ were assigned to the enolic species absorbed on the surface of $Ag/Al_2O_3$. This assignment was confirmed by using 2,3-dihydrofuran as an enolic model compound in our DRIFTS study, which has C=C bonded with an oxygen structure. A similar feature

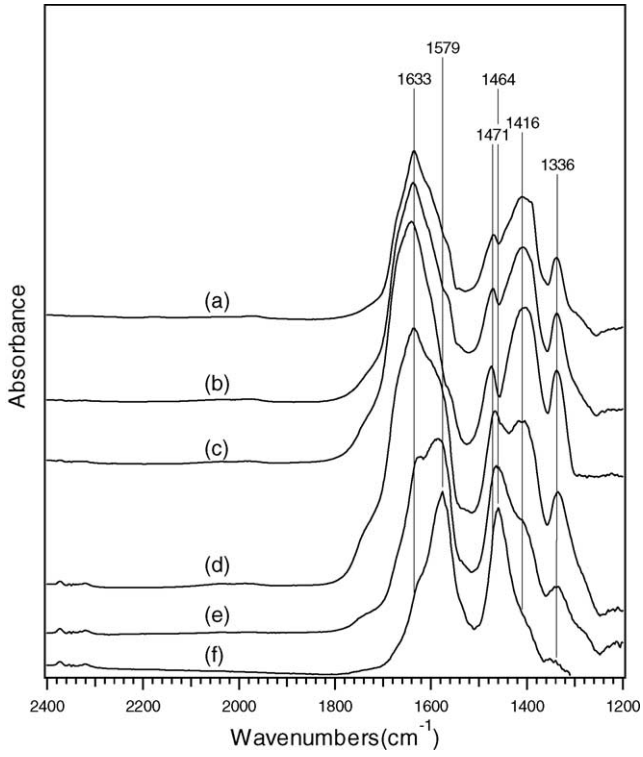


Fig. 6. In situ DRIFTS spectra of adsorbed species in steady states on $Ag/Al_2O_3$ in a flow of $C_2H_5OH + O_2$ at (a) 200 °C, (b) 250 °C, (c) 300 °C, (d) 400 °C, (e) 500 °C and (f) 600 °C. Conditions: 1565 ppm $C_2H_5OH$, 10 vol.% $O_2$ /$N_2$ [38].

strongly supported our assignment: the surface enolic species was observed on $Ag/Al_2O_3$. From a comparison of the intensity of each peak in Fig. 6, we deduced that the enolic species is predominant during the oxidation of $C_2H_5OH$ on the $Ag/Al_2O_3$ surface at low temperatures (within the range of 200–400 °C). However, at high temperatures ranging from 500 to 600 °C, the surface acetate species becomes dominant. In addition, our TPD experiments show the evidences for $C_4$ surface enolic species [41]. This indicates that a condensation reaction occurs synchronously during the partial oxidation of $C_2H_5OH$ over $Ag/Al_2O_3$, which leads to chain growth of desorption products. The condensation reactions of aldehydes, as well as of ketones, are widely used in organic synthesis and are commonly catalyzed by zeolites, $Al_2O_3$, and $TiO_2$ [54–58].

Density functional theory (DFT) calculations were also used to confirm the structure of adsorbed enolic species on $Ag/Al_2O_3$ using the Gaussian 98 suite of programs. The simulation molecular structure model and FTIR spectrum of the surface enolic species on $Ag/Al_2O_3$ are shown in Fig. 7. In model A, the enolic species ($CH_2$═$CH$–$O^-$) bonded with a silver atom, and the optimized distance between the oxygen and silver atom was 2.072 Å. Apparently, the calculated FTIR spectrum was reasonably similar to the corresponding experimental result. The asymmetric stretching vibration mode of the enolic species was calculated at 1645 $cm^{-1}$ with a relatively high infrared intensity of 61 km $mol^{-1}$, which is 12 $cm^{-1}$ higher than the experimental harmonic frequency (1633 $cm^{-1}$). Compared to the experimental value, the calculated symmetric stretching vibrational mode of this species varied within less than 13 $cm^{-1}$ (1429 $cm^{-1}$ against 1416 $cm^{-1}$). The calculated C–H deformation vibration mode (1328 $cm^{-1}$) was 8 $cm^{-1}$ lower than the experimental one (1336 $cm^{-1}$). For model B ($CH_2$═$CH_2$–$CH$═$CH$–O–Al–Ag), the calculated FTIR spectrum was also reasonably similar to the corresponding experimental one (see Figs. 6 and 7D).

Thirty-two models of adsorbed species were calculated. Different kinds of adsorbed species and the interaction of the surface with the adsorbed species were considered. However, only the enolic species' DFT calculations were in good agreement with the experimental value. On the basis of this result, we concluded that there is excellent agreement between the calculational vibration spectrum and the experimental spectrum, supporting our assignment of the structure of surface enolic species. Furthermore, a surface reaction mechanism was proposed for the formation of enolic species as shown in Scheme 1.

### 3.2. Reactivity of enolic species

The reactivity of the enolic species toward $NO + O_2$ was evaluated by the in situ DRIFTS method. As shown in Fig. 8, after $Ag/Al_2O_3$ was exposed to $C_2H_5OH + O_2$ for 60 min (curve a), very strong peaks assignable to the absorbed enolic species (1633, 1416 and 1336 $cm^{-1}$), and acetate peaks (1579 and 1464 $cm^{-1}$) were observed. Switching the fed gas to $NO + O_2$ resulted in a sharp decrease in the intensity of enolic species peaks accompanied by a corresponding increase in the intensity of a new NCO peak at 2229 $cm^{-1}$ [16,17,50], indicating that the enolic species contributes to the formation of NCO species. It is widely accepted that the NCO species could be a crucial intermediate in the SCR of $NO_x$ over $Ag/Al_2O_3$, and its high productivity results in high efficiency of $NO_x$ reduction by $C_2H_5OH$ or hydrocarbons [19,48,59,60]. Since the enolic species plays an important role in NCO species formation, this species must also be another crucial intermediate in the SCR of $NO_x$ by $C_2H_5OH$.

Many research groups have studied the formation and reactivity of acetate during $NO + C_3H_6 + O_2$ reactions on oxide catalysts and metal-supported catalysts such as $Al_2O_3$ [61,62] and $Ag/Al_2O_3$ [7], and have suggested that acetate, as a dominant adsorbed species at high temperatures, plays a crucial role in the formation of NCO species by reacting toward $NO + O_2$. The reaction can be described as follows: $NO + O_2 + C_3H_6 \rightarrow NO_x$ (nitrate in particular) + $C_xH_yO_z$ (acetate in particular) $\rightarrow$ R–$NO_2$ + R–ONO $\rightarrow$ –NCO + –CN + NO + $O_2 \rightarrow N_2$. In the case of the SCR of $NO_x$ by $C_2H_5OH$ over $Ag/Al_2O_3$, Kameoka et al. [50] proposed that acetate also plays a key role in NCO species formation. Furthermore, they considered that more acetate and less

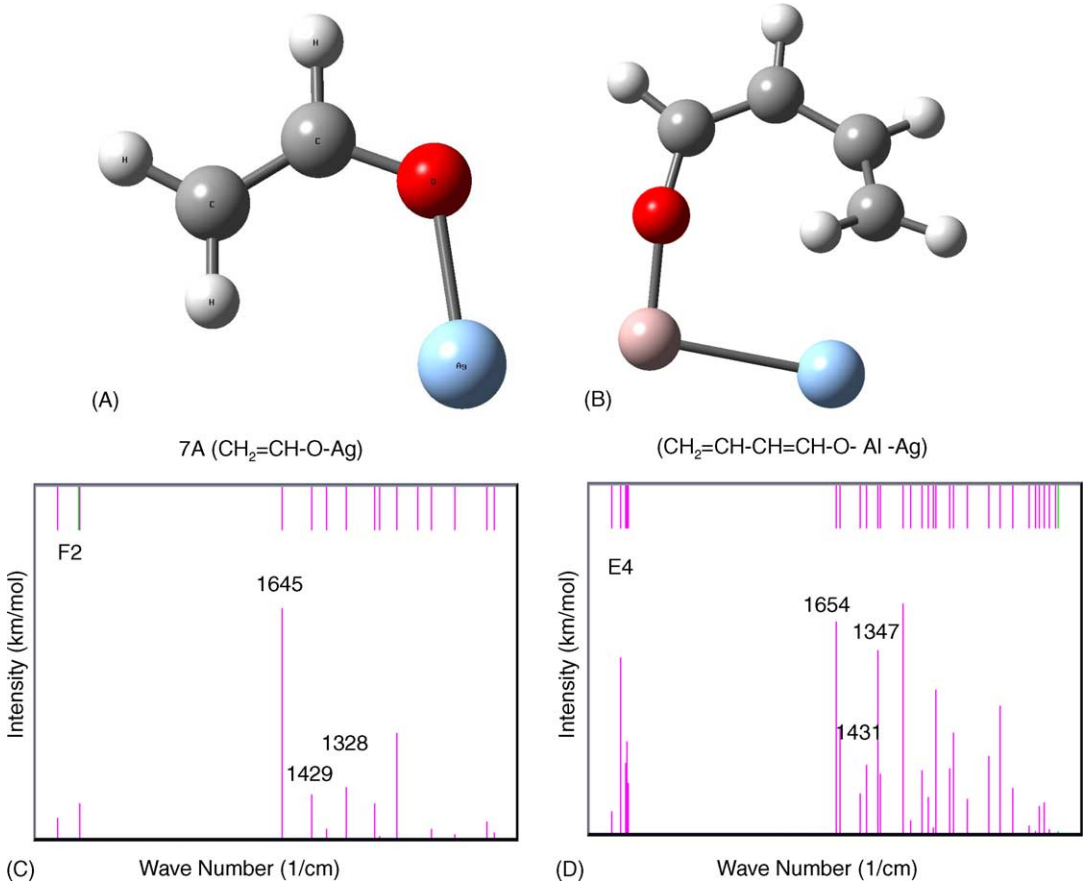


Fig. 7. Molecular structure and optimized geometries of the calculational model for absorbed enolic species from $C_2H_5OH$ on $Ag/Al_2O_3$ by oxidation (A) and aldol condensation (B); (C) and (D) calculated vibrational IR spectra for models A and B at the DFT-B3P86/LANL2DZ level [38,41].

nitrates were observed in comparison with the SCR of $NO_x$ by $C_3H_6$, which probably explains why NCO species is more easily produced when $C_2H_5OH$ is used as a reductant. If the acetate really plays a crucial role in NCO species formation during the SCR of $NO_x$ by $C_2H_5OH$, it should have high reactivity with $NO + O_2$. However, as shown in Fig. 8(B), enolic species have much higher reactivity than acetate on $Ag/Al_2O_3$ towards $NO + O_2$ to form NCO species. Actually, the acetate did not react with $NO + O_2$ until the enolic species had nearly disappeared from the $Ag/Al_2O_3$ surface.

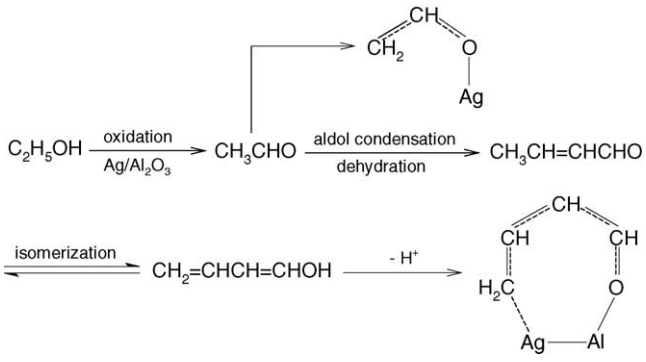


Scheme 1. The formation of an adsorbed enolic species on $Ag/Al_2O_3$.

This means that enolic species, instead of acetate, play a crucial role in the $NO_x$ reduction by $C_2H_5OH$.

### 3.3. Reaction pathway of the SCR of $NO_x$ by $C_2H_5OH$ over $Ag/Al_2O_3$

Fig. 9 shows the DRIFTS spectra of $Ag/Al_2O_3$ during the $NO + C_2H_5OH + O_2$ reaction at various temperatures (200–550 °C) in a steady state. Surface species such as enolic species (1633, 1416 and 1336 $cm^{-1}$), acetate (1572 $cm^{-1}$ and 1473–1462 $cm^{-1}$), and NCO (2229 $cm^{-1}$) were found. In addition, strong peaks at 1583, 1302 $cm^{-1}$ and shoulders at 1612, 1560 and 1250 $cm^{-1}$ were also observed, which were respectively assigned to unidenate (1560 $cm^{-1}$), bidentate (1583, 1302 $cm^{-1}$), and bridging (1612 $cm^{-1}$) nitrates according to the literature [31,50]. Kameoka et al. [50] reported that these nitrates were highly active in their reaction with $C_2H_5OH + O_2$ to form NCO species, which was also supported by our earlier study [38]. The intensity of each peak indicated that the enolic species and the nitrates are predominant at 200 °C. Heating the sample causes the intensity of the peaks to decrease for these two types of adsorbed species. In contrast, a sharp increase in the intensity of the NCO peak (2229 $cm^{-1}$) was observed. At 450 °C, the NCO

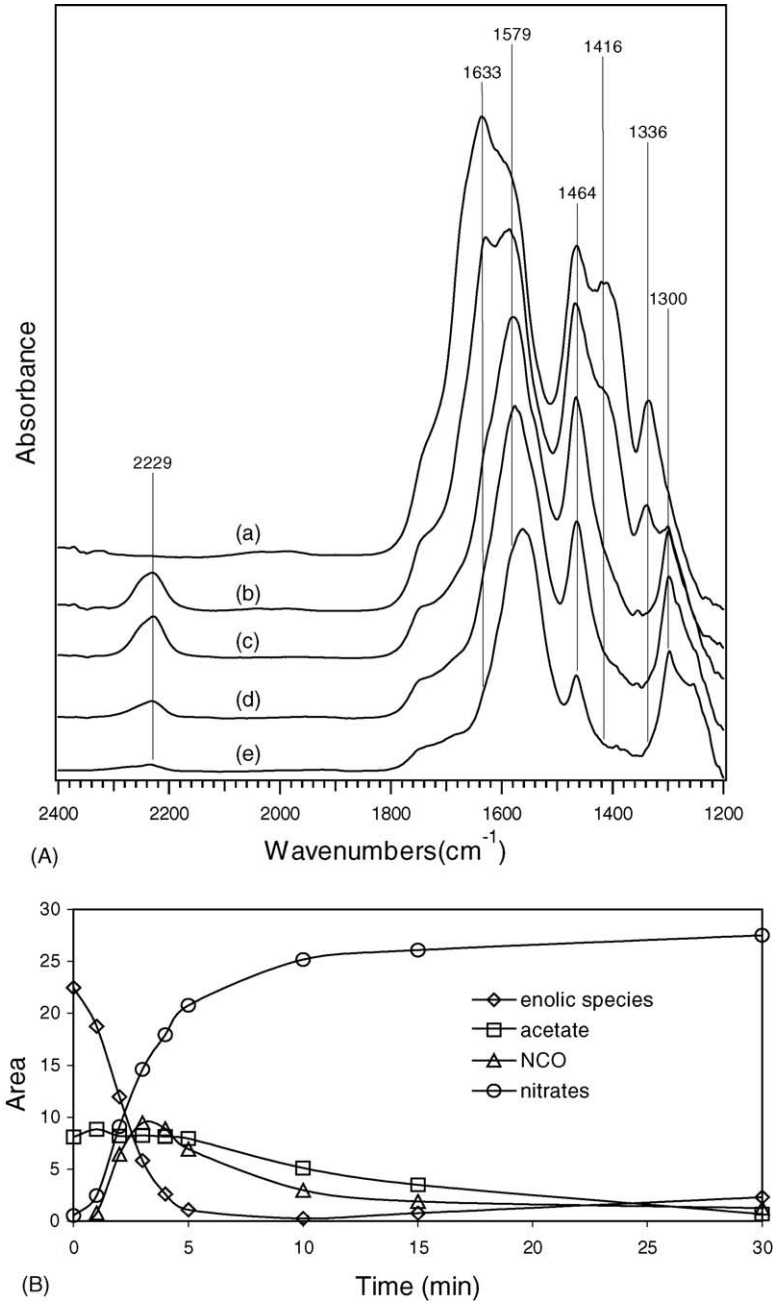


Fig. 8. (A) Dynamic changes of in situ DRIFTS spectra on $Ag/Al_2O_3$ as a function of time in a flow of NO + $O_2$ at 400 °C. Before measurement, the catalyst was pre-exposed to a flow of $C_2H_5OH$ + $O_2$ for 60 min at 400 °C (a), in a flow of NO + $O_2$ (b) 1 min, (c) 5 min, (d) 10 min and (e) 30 min. (B) Time dependence of the integrated areas of the peak in the range of 2160–2305 $cm^{-1}$ ((Δ), NCO), 1612–1711 $cm^{-1}$ ((◇), enolic species), 1439–1508 $cm^{-1}$ ((□), acetate) and 1209–1321 $cm^{-1}$ ((○), nitrates). Conditions: 800 ppm NO, 1565 ppm $C_2H_5OH$, 10 vol.% $O_2$ /$N_2$. [38].

peak reached a maximum, while the peaks of enolic species and nitrates became very weak at this temperature. Heating the sample in sequential increments to a final temperature of 550 °C, the enolic species and nitrate peaks were barely perceptible, and acetate became the predominant surface species. These results strongly suggest that the enolic species and nitrates are key intermediates in the formation of NCO species during the SCR of $NO_x$ by $C_2H_5OH$ over $Ag/Al_2O_3$.

Taking our earlier works [16,17,36–45] into account, we proposed a mechanism for the $NO_x$ reduction by $C_2H_5OH$, which can be described by a simplified reaction scheme, as shown in Scheme 2. The reaction starts with the formation of both adsorbed nitrates via NO oxidation by $O_2$ and enolic species and acetate via the partial oxidation of $C_2H_5OH$ over $Ag/Al_2O_3$. The reaction between the two kinds of adsorbed species then leads to the formation of NCO species directly, or via organo-nitrogen compounds (such as R–ONO and R–$NO_2$), which is widely accepted in studies of the SCR of $NO_x$ [7,16,47,50,63]. Subsequently, NCO species reacts with NO + $O_2$ and nitrates to yield $N_2$. It should be pointed out

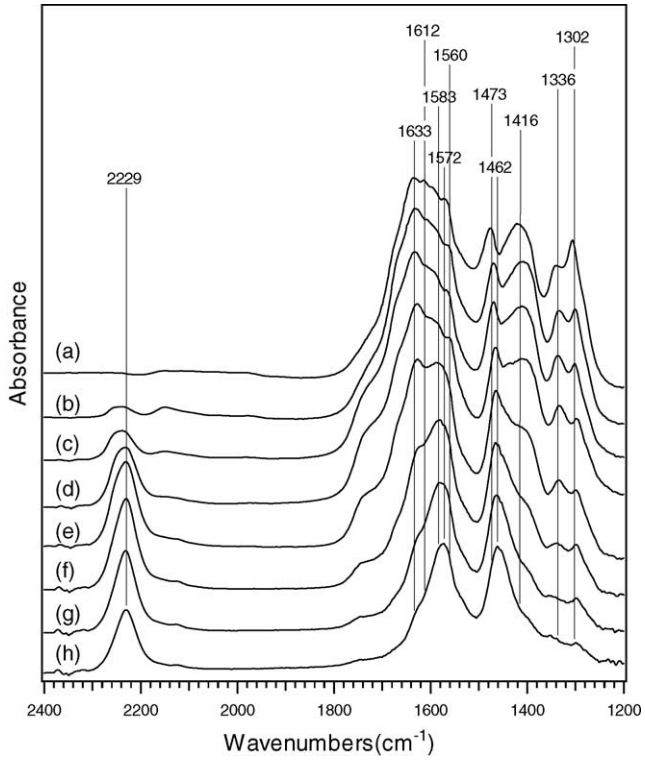


Fig. 9. In situ DRIFTS spectra of adsorbed species in steady states over $Ag/Al_2O_3$ in a flow of NO + $C_2H_5OH$ + $O_2$ at (a) 200 °C, (b) 250 °C, (c) 300 °C, (d) 350 °C, (e) 400 °C, (f) 450 °C, (g) 500 °C and (h) 550 °C. Conditions: 800 ppm NO, 1565 ppm $C_2H_5OH$, 10 vol.% $O_2$ /$N_2$ [41].

that the acetate formed by the reaction of $C_2H_5OH$ + $O_2$ also reacts toward NO + $O_2$ to produce NCO species. However, the relatively low activity of acetate toward NO + $O_2$ results in this parallel reaction not playing an important role in the formation of NCO species.

The enolic species has a higher reactivity with NO + $O_2$ on $Ag/Al_2O_3$ than acetate has, and the former is the main surface species during the partial oxidation of $C_2H_5OH$ over $Ag/Al_2O_3$. As a result, high surface concentration of NCO species and high efficiency of $NO_x$ reduction are obtained when $C_2H_5OH$ is used as a reductant during the SCR of NOx. We also studied the partial oxidation of $C_3H_6$ and the SCR of $NO_x$ by $C_3H_6$ over $Ag/Al_2O_3$. In both cases, only a small amount of enolic species was formed, accompanied by the formation of large amounts of acetate. This relates to a lower NCO species concentration over $Ag/Al_2O_3$ as well as relatively lower $NO_x$ conversion when $C_3H_6$ is used as a reductant.

### 3.4. Influence of water vapor on the SCR of $NO_x$ by $C_2H_5OH$ over $Ag/Al_2O_3$

In general, the SCR of $NO_x$ by hydrocarbons is suppressed in the presence of water vapor, which makes utilization of the catalysts difficult because great amounts of water vapor inevitably exist in various exhausts. When $C_2H_5OH$ is used as a reductant, however, $Ag/Al_2O_3$ was extremely effective in the $NO_x$ reduction even in the presence of water vapor [10,11,17]. Our results showed that the addition of water vapor enhances the $NO_x$ reduction by $C_2H_5OH$ over $Ag/Al_2O_3$, especially in the low temperature range (Fig. 5). Up to now, however, the mechanism behind water vapor's influence on the SCR of $NO_x$ by $C_2H_5OH$ is still unclear.

Fig. 10 shows the influence of water vapor on the $NO_x$ reduction by $C_2H_5OH$ over $Ag/Al_2O_3$ at 300 °C. In the absence of water vapor, NCO species (2237 $cm^{-1}$), enolic species (1633, 1416 and 1336 $cm^{-1}$), acetate (1576 and 1470 $cm^{-1}$), and nitrate (1564 and 1304 $cm^{-1}$) were observed. It is apparent that the addition of water vapor inhibited the formation of acetate, while the concentration of enolic species changed little on the $Ag/Al_2O_3$ surface. Considering that the formation of enolic species is parallel to the formation of acetate and that the two intermediates compete for adsorption sites, a decrease in the concentration of acetate on $Ag/Al_2O_3$ means more adsorption sites are available for the enolic species formation and its subsequent reaction. As a consequence, the reaction of NCO species to form $CO_2$ was enhanced. This was confirmed by both a decrease in the concentration of NCO species and an increase in the intensity of gas phase $CO_2$

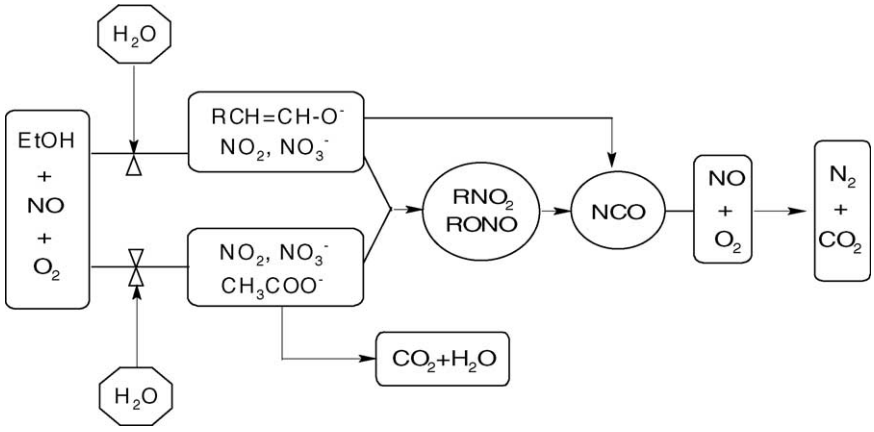


Scheme 2. A possible reaction mechanism of the SCR of $NO_x$ by $C_2H_5OH$ over $Ag/Al_2O_3$.

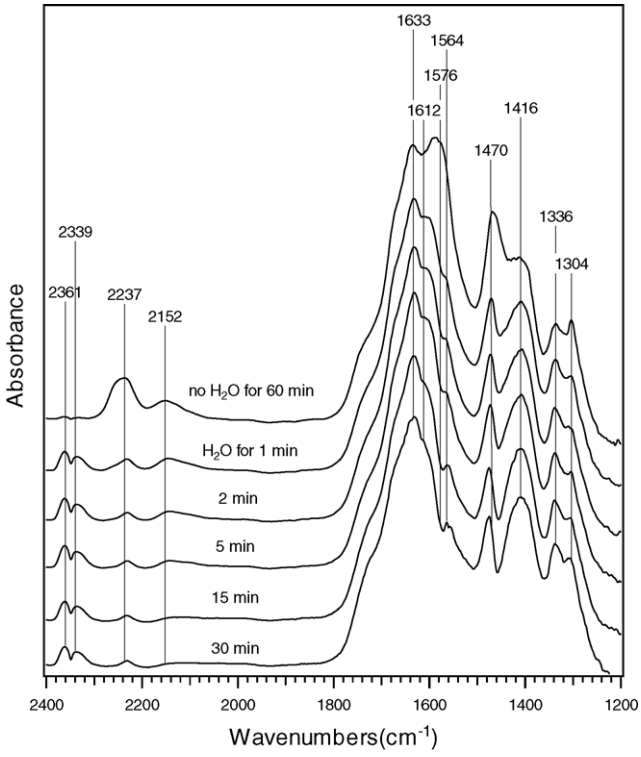


Fig. 10. Dynamic changes of in situ DRIFTS spectra in the flow of $NO + O_2 + C_2H_5OH + H_2O$ over $Ag/Al_2O_3$ at 300 °C after exposure to $NO + O_2 + C_2H_5OH$ for 60 min. Conditions: 800 ppm NO, 1565 ppm $C_2H_5OH$, 10 vol.% $O_2/N_2$, 0 or 10 vol.% $H_2O$.

peaks (2361 and 2339 $cm^{-1}$). Since the formation of enolic species and its subsequent reaction play a dominant role in the SCR of $NO_x$ by $C_2H_5OH$ over $Ag/Al_2O_3$, it is reasonable to conclude that the presence of water vapor enhances this process as shown in Scheme 2 which has been proved by activity test in Fig. 5.

## 4. Improvement of the low temperature activity and sulphur tolerance of $Ag/Al_2O_3$

At the low temperature range, $Ag/Al_2O_3$ is not active for the SCR of $NO_x$ by $C_3H_6$, and extensive studies have been performed focusing on this. He et al. first reported at the 69th Annual Meeting of JCS [64] that the SCR of $NO_x$ by $C_3H_6$ over an $Ag/Al_2O_3$ catalyst was effectively enhanced by co-impregnating with a small amount of Pd, whereas it was reduced by the addition of Pt and Au. The effect of adding Pd on Ag/mordenite was also reported by Masuda et al. [65] using $(CH_3)_2O$ as a reductant, although the durability of Ag/Pd/mordenite decreased in the presence of water vapor. Seker et al. [66] showed the negative effect of Au on $Ag/Al_2O_3$ for the NO xreduction with $C_3H_6$. In our earlier study [37], we reported that the addition of trace Pd (0.01 wt.%) to $Ag/Al_2O_3$ is favorable for the partial oxidation of $C_3H_6$ to form enolic species, resulting in an increase in $NO_x$ conversion.

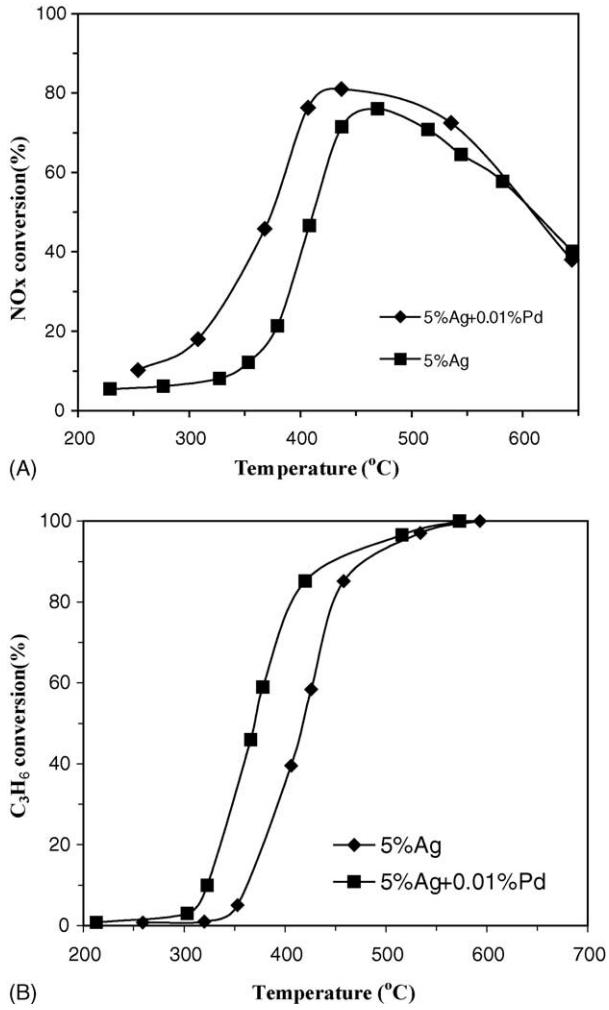


Fig. 11. (A) Catalytic activity for $NO_x$ reduction by $C_3H_6$ over $Ag/Al_2O_3$ and $Ag–Pd/Al_2O_3$ catalysts respectively at various temperatures in the presence of water vapor. (B) Conversions of $C_3H_6$ into $CO_x$ over $Ag–Pd/Al_2O_3$ and $Ag/Al_2O_3$ respectively at various temperatures in the presence of water vapor. Conditions: 800 ppm NO, 1714 ppm $C_3H_6$, 10 vol.% $O_2/N_2$, 10 vol.% $H_2O$, catalyst weight = 1.2 g, $W/F = 0.018$ g s $cm^{-3}$ [37].

Fig. 11(A) shows the SCR of $NO_x$ over $Ag/Al_2O_3$ and $Ag–Pd/Al_2O_3$ catalysts by $C_3H_6$ at various temperatures. Both $NO_x$ conversions increased with increase in the reaction temperature and reached a maximum at 437 °C for $Ag–Pd/Al_2O_3$ and at 470 °C for $Ag/Al_2O_3$. The $NO_x$ conversions then decreased with further increases in the reaction temperature. The highest rate of $NO_x$ conversion was 82% over $Pd–Ag/Al_2O_3$, which was higher than the 73% rate over $Ag/Al_2O_3$. Obviously, a trace amount of Pd added into $Ag/Al_2O_3$ can enhance the $NO_x$ conversion in the presence of excess oxygen and water vapor. This effect of adding metals is considered to be favorable for activating reductant molecules, for example, the scission of a C–C bond and partial oxidation. Fig. 11(B) shows the conversions of $C_3H_6$ into $CO_x$ over $Pd–Ag/Al_2O_3$ and $Ag/Al_2O_3$. Similar to $NO_x$ conversion, the curve of $C_3H_6$ conversion for $Ag/Al_2O_3$ shifted to lower temperatures after the addition of Pd.

This result suggests that Ag–Pd/$Al_2O_3$ can activate $C_3H_6$ to react with NO + $O_2$.

According to the tests using Ag–Pd/$Al_2O_3$ catalysts and contrastive Ag/$Al_2O_3$, we found that loading trace amounts of Pd on Ag/$Al_2O_3$ led to a significant improvement of $NO_x$ conversion during the SCR of $NO_x$ by $C_3H_6$, especially at low temperatures. In situ DRIFTS results suggested that Pd addition catalyzes the partial oxidation of $C_3H_6$ into a surface enolic species, and the surface enolic species is quite reactive towards $NO_3^-$ and $NO_2$ to form surface NCO species. This is in good agreement with the new reaction mechanism proposed above.

As $SO_2$ usually exists in lean-burn engine exhaust, the sulphur tolerance of oxide and base metal catalysts has been widely investigated [67]. An inhibition of the SCR of $NO_x$ by $SO_2$ was observed in essentially all cases, originating from the reaction among $SO_2$, $O_2$ and the catalyst surface to form thermodynamically stable sulphate phases under reaction conditions [27]. The formation of these sulphate species brings about a reduction in the number of 'strong' chemisorption sites for $NO_x$ [28,68]. Our results showed that Ag/$Al_2O_3$ is highly effective for the SCR of $NO_x$ by $C_3H_6$ even in the presence of $SO_2$, while the addition of Pd to this catalyst results in an obvious loss in activity, especially in the low temperature range. On the other hand, our results demonstrated that $Ag_2SO_4$/$Al_2O_3$ performs well in $NO_x$ reduction; thus the formation of some aluminum sulphate phases might be responsible for the activity loss [7]. Based on this prediction, we attempted to enhance the sulphur tolerance of Ag–Pd/$Al_2O_3$ by modifying the supporter to reduce the adsorption and accumulation of sulphate species, a technique which was also supported by our recent experiments [69]. Furthermore, DRIFTS spectra suggested that the presence of $SO_2$ inhibited the formation of enolic species and NCO species, which are the key intermediates of the SCR of $NO_x$ by $C_3H_6$ over Ag–Pd/$Al_2O_3$.

Burch [7] reported that the inhibition extent of the SCR of $NO_x$ by $SO_2$ is dramatically dependent on the nature of the reductant and the $SO_2$ concentration. When using alcohols as reductants, the loss in activity due to $SO_2$ is usually only a limited fraction of the initial activity [70]. We also observed similar phenomena during the $NO_x$ reduction by $C_2H_5OH$ over Ag/$Al_2O_3$. In addition, our DRIFTS results showed that the presence of $SO_2$ hardly changed the formation of enolic species originating from the partial oxidation of $C_2H_5OH$, which probably explains why the inhibition of $SO_2$ largely depends on the nature of the reductant.

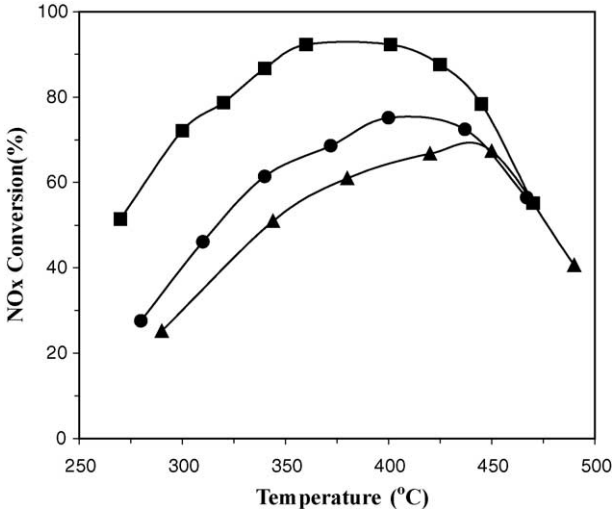


Fig. 12. Activity of Ag/$Al_2O_3$ for the SCR of $NO_x$ by $C_2H_5OH$ on an actual engine bench (GHSV: (■) 30,000, (●) 50,000 and (▲) 80,000).

As discussed above, Ag/$Al_2O_3$ is a promising candidate for the $NO_x$ reduction from diesel engine exhaust. However, Eränen et al. [35] noticed that a considerable amount of CO was produced during the SCR of NO with octane over Ag/$Al_2O_3$. In their study, a commercial Pt-oxidation catalyst was extremely effective for the removal of CO when placed after Ag/$Al_2O_3$, while a drastic decrease of $NO_x$ conversion was observed. We also found that a large amount of CO was produced during the $NO_x$ reduction by either propene or

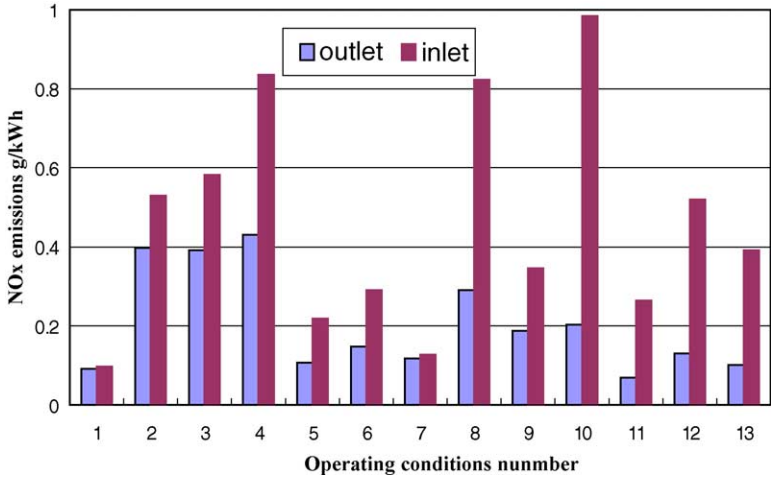


Fig. 13. Performance of $NO_x$ catalytic converter in the European Economic Community's 13-mode test cycle.

Table 2
$NO_x$ emission and EURO standards

| Average $NO_x$ emission (g $kW^{-1}$ h) | Initial outlet | Catalytic converter outlet | $NO_x$ conversion | Euro III standard | Euro IV standard |
|---|---|---|---|---|---|
| $NO_x$ (steady state) | 5.82 | 1.74 | 70.0% | 5.0 | 3.5 |
| $NO_x$ (transient state) | 6.02 | 2.67 | 55.6% | 5.0 | 3.5 |

ethanol over $Ag/Al_2O_3$. In order to eliminate undesired by-products, a two-component composite catalyst, $Ag/Al_2O_3 + Cu/Al_2O_3$, was employed, which was proved to be quite effective for both $NO_x$ reduction and CO removal. In addition, it has been reported that a substantial amount of nitrogen-containing by-products such as $N_2O$, $NH_3$, $CH_3CN$, and HCN are produced during the SCR of $NO_x$ by $C_2H_5OH$ over $Ag/Al_2O_3$. Further studies are planned to attempt to develop the composite catalyst system, combining placing an oxidation catalyst behind the $Ag/Al_2O_3$, to remove these nitrogen-containing by-products without losing any activity of the SCR of $NO_x$ by $C_2H_5OH$.

## 5. Diesel $NO_x$ reduction test with an actual engine bench

The results shown in Fig. 12 demonstrate that the $Ag/Al_2O_3$–$C_2H_5OH$ system was extremely effective for the $NO_x$ reduction on a four-cylinder direct injection engine bench [71]. At the typical diesel engine exhaust temperature range, the conversion of $NO_x$ remained rather high at each space velocity tested (GHSV: 30,000, 50,000 and 80,000 $h^{-1}$). In the case of a space velocity of 30,000 $h^{-1}$, the light-off temperature of $NO_x$ conversion was 270 °C and the highest $NO_x$ conversion reached 92.3% at an operating temperature of 400 °C ($C_2H_5OH/NO_x$ = 3:1 on a mass basis). This result was similar to our results of the laboratory scale test, indicating the most realistic potential in reducing $NO_x$ under real diesel engine exhaust conditions.

Our $Ag/Al_2O_3$–$C_2H_5OH$ NOx catalytic converter satisfied the $NO_x$ emission requirements of the Euro III standard using the European Economic Community's 13-mode test cycle (Fig. 13). Table 2 shows the average $NO_x$ emission of diesel engines with and without de-$NO_x$ catalytic converter aftertreatment. It is obvious that the $NO_x$ emission from a diesel engine, which was at the level of Euro II, was greatly improved, meeting the requests for the Euro III standard by the use of a catalytic converter. In fact, the average $NO_x$ emission on the catalytic converter outlet also satisfied the requirements for the Euro IV standard.

## 6. Continuing and future work

Diesel engines have a number of advantages including a high power/weight ratio, more than 50% thermal efficiency, infrequent engine problems, and high fuel economy. However, the nitrogen oxides ($NO_x$) and particulate matter (PM) emitted from diesel engines constitute two major air pollution sources. Our previous research focused on the $NO_x$ reduction in lean-burn exhausts. Our recently results showed that using Ethanol–diesel blend fuel could greatly reduce the PM emission [71,72]. Ethanol–diesel blend fuel partly replaces petroleum with a renewable resource and it is a promising alternative fuel for diesel engines. Therefore, employing the Ethanol–diesel blend fuel with our $Ag/Al_2O_3$–$C_2H_5OH$ $NO_x$ catalytic converter can reduce $NO_x$ and PM emissions in diesel engine exhaust simultaneously.

In the near future, we plan to make further attempts to optimize the blend of Ethanol–diesel fuels and develop a corresponding catalytic converter system for reducing both $NO_x$ and PM in diesel engine exhaust. The Ethanol–diesel blend fuel and corresponding $NO_x$ catalytic converter systems will first be demonstrated on the urban transit system of buses, which is considered a major source of air pollution in urban regions.

## Acknowledgments

This work was partially supported by the Innovation Program of the Chinese Academy of Sciences (KZCX3-SW-430). The authors are grateful to Changbin Zhang, Jin Wang, Hongwei Gao, Junfeng Liu, Xiaoyan Shi and Shuxia Xie for their contributions to this work. The authors would like to acknowledge the help of Professor Jianxin Wang and Professor Shijin Shuai (Tsinghua University) for the diesel engine experiments.

## References

[1] F. Nakajima, Catal. Today 10 (1991) 1.
[2] N.-Y. Topsoe, Cattech 1 (1997) 125.
[3] A. Fritz, V. Pitchon, Appl. Catal. B 13 (1997) 1.
[4] R.M. Heck, Catal. Today 53 (1999) 519.
[5] M. Shelef, Cham. Rev. 95 (1995) 209.
[6] Y. Traa, B. Burger, J. Weitkamp, Micropor. Mesopor. Mater. 30 (1999) 3.
[7] R. Burch, J.P. Breen, F.C. Meunier, Appl. Catal. B 39 (2002) 283.
[8] A. Satsuma, K. Shimizu, Prog. Energy Combus. Sci. 29 (2003) 71.
[9] T. Miyadera, K. Yoshida, Chem. Lett. 2 (1993) 1483.
[10] T. Miyadera, Appl. Catal. B 2 (1993) 199.
[11] T. Miyadera, Appl. Catal. B 13 (1997) 157.
[12] M.C. Kung, K.A. Bethke, J. Yan, J.-H. Lee, H.H. Kung, Appl. Surf. Sci. 121–122 (1997) 261.
[13] M. Haneda, Y. Kintaichi, M. Inaba, H. Hamada, Appl. Surf. Sci. 121–122 (1997) 391.
[14] T.E. Hoost, R.J. Kudla, K.M. Collins, M.S. Chattha, Appl. Catal. B 13 (1997) 59.
[15] K.A. Bethke, H.H. Kung, J. Catal. 172 (1997) 93.
[16] S. Sumiya, H. He, A. Abe, N. Takezawa, K. Yoshida, J. Chem. Soc., Faraday Trans. 94 (1998) 2217.
[17] S. Sumiya, M. Saito, H. He, Q.-C. Feng, N. Takezawa, Catal. Lett. 50 (1998) 87.
[18] M. Handea, Y. Kintaichi, M. Inaba, H. Hamada, Catal. Today 42 (1998) 127.

[19] S. Kameoka, D. Chafik, Y. Ukisu, T. Miyadera, Catal. Lett. 55 (1998) 211.
[20] T. Nakatsuji, R. Yasukawa, K. Tabata, K. Ueda, M. Niwa, Appl. Catal. B 17 (1998) 333.
[21] H.-W. Jen, Catal. Today 42 (1998) 37.
[22] Y. Yamashita, N. Aoyama, N. Takezawa, K. Yoshida, J. Mol. Catal. A 150 (1999) 233.
[23] N. Aoyama, Y. Yamashita, A. Abe, N. Takezawa, Phys. Chem. Chem. Phys. 1 (1999) 3365.
[24] F.C. Meunier, J.P. Breen, V. Zuzaniuk, M. Olsson, J.R.H. Ross, J. Catal. 187 (1999) 493.
[25] A. Martínez-Arisa, M. Fernández-García, A. Iglesias-Juez, J.A. Anderson, J.C. Conesa, J. Soria, Appl. Catal. B 28 (2000) 29.
[26] K. Shimizu, A. Satsuma, T. Hattori, Appl. Catal. B 25 (2000) 239.
[27] F.C. Meunier, J.R.H. Ross, Appl. Catal. B 24 (2000) 23.
[28] F.C. Meunier, V. Zuzaniuk, J.P. Breen, M. Olsson, J.R.H. Ross, Catal. Today 59 (2000) 287.
[29] M.C. Kung, H.H. Hung, Topic Catal. 10 (2000) 21.
[30] F.C. Meuiner, R. Ukropec, C. Stapleton, J.R.H. Ross, Appl. Catal. B 30 (2001) 163.
[31] K. Shimizu, J. Shibata, H. Yoshida, A. Satsuma, T. Hattori, Appl. Catal. B 30 (2001) 151.
[32] G.W. Busser, O. Hinrichsen, M. Muhler, Catal. Lett. 79 (2002) 49.
[33] T. Furusawa, L. Lefferts, K. Seshan, K. Aika, Appl. Catal. B 42 (2003) 25.
[34] A. Iglesias-Juez, A.B. Hungría, A. Martínez-Arias, A. Fuerte, M. Fernández- García, J.A. Anderson, J.C. Conesa, J. Soria, J. Catal. 217 (2003) 310.
[35] K. Eränen, L.-E. Lindfors, F. Klingstedt, D.Y. Murzin, J. Catal. 219 (2003) 25.
[36] Y. Yu, H. He, Q. Feng, J. Phys. Chem. B 107 (2003) 13090.
[37] H. He, J. Wang, Q. Feng, Y. Yu, K. Yoshida, Appl. Catal. B 46 (2003) 365.
[38] Y. Yu, H. He, Q. Feng, H. Gao, X. Yang, Appl. Catal. B 49 (2004) 159.
[39] H. He, C. Zhang, Y. Yu, Catal. Today 90 (2004) 191.
[40] J. Wang, H. He, Q. Feng, Y. Yu, K. Yoshida, Catal. Today 93–95 (2004) 783.
[41] Y.B. Yu, H.W. Gao, H. He, Catal. Today 93–95 (2004) 805.
[42] Y. Yu, H. He, J. Chin. Catal. 24 (2003) 385.
[43] H. He, R. Zhang, Y. Yu, J. Liu, J. Chin. Catal. 24 (2003) 788.
[44] H. He, R. Zhang, Y. Yu, J. Liu, J. Chin. Catal. 25 (2004) 460.
[45] C. Zhang, H. He, Y. Yu, R. Zhang, Chem. J. Chin. U. 25 (2004) 136.
[46] K. Takagi, T. Kobayashi, H. Ohkita, T. Mizushima, N. Kakuta, A. Abe, K. Yoshida, Catal. Today 45 (1998) 123.
[47] T. Chafik, S. Kameoka, Y. Ukisu, T. Miyadera, J. Molecular Catal. A 136 (1998) 203.
[48] S. Kameoka, T. Chafik, Y. Ukisu, T. Miyadera, Catal. Lett. 51 (1998) 11.
[49] T. Miyadera, Appl. Catal. B 16 (1998) 155.
[50] S. Kameoka, Y. Ukisu, T. Miyadera, Phys. Chem. Chem. Phys. 2 (2000) 367.
[51] N. Bion, J. Saussey, M. Haneda, M. Daturi, J. Catal. 217 (2003) 47.
[52] R.W.G. Wyckoff, Am. J. Sci. 3 (1922) 184.
[53] B. Stehlik, P. Weidenthaler, Collect. Czech. Chem. Commun. 24 (1959) 1416.
[54] K. Kubelková, J. Čejka, J. Nováková, Zeolites 11 (1991) 48.
[55] A.I. Biaglow, J. Šepa, R.J. Gorte, D. White, J. Catal. 151 (1995) 373.
[56] A. Panov, J.J. Fripiat, Langmuir 14 (1998) 3788.
[57] M. El-Maazawi, A.N. Finken, A.B. Nair, V.H. Grassian, J. Catal. 191 (2000) 138.
[58] M.I. Zaki, M.A. Hasan, F.A. Al-Sagheer, L. Pasupulety, Langmuir 16 (2000) 430.
[59] Y. Ukisu, S. Sato, G. Muramatsu, K. Yoshida, Catal. Lett. 11 (1991) 177.
[60] Y. Ukisu, S. Sato, A. Abe, K. Yoshida, Appl. Catal. B 2 (1993) 147.
[61] K. Shimizu, H. Kawabata, A. Satuma, T. Hattori, Appl. Catal. B 19 (1998) 87.
[62] K. Shimizu, H. Kawabata, A. Satsuma, T. Hattori, J. Phys. Chem. B 103 (1999) 5240.
[63] T. Tanaka, T. Okuhara, M. Misono, Appl. Catal. B 4 (1994) 1.
[64] H. He, N. Irite, K. Onai, K. Yoshida, Proceedings of the 69th Annual Meeting of Chem. Soc. Jpn., A314.
[65] K. Masuda, K. Shinoda, T. Kato, K. Tsujimura, Appl. Catal. B 15 (1998) 29.
[66] E. Seker, J. Cavataio, E. Gulari, P. Lorpongpaiboon, S. Osuwan, Appl. Catal. A 183 (1999) 121.
[67] M.C. Kung, P.W. Park, D.W. Kim, H.H. Kung, J. Catal. 181 (1999) 1.
[68] R. Burch, E. Halpin, J.A. Sullivan, Appl. Catal. B 17 (1998) 115.
[69] J. Wang, H. He, S. Xie, Y. Yu, Catal. Commun., in press.
[70] M. Tabata, H. Tsuchida, K. Miyamoto, T. Yoshinari, H. Yamazaki, Y. Kintaichi, M. Sasaki, T. Ito, H. Hamada, Appl. Catal. B 6 (1995) 169.
[71] B.-Q. He, S.-J. Shuai, J.-X. Wang, H. He, Atmos. Environ. 37 (2003) 4965.
[72] R. Zhang, H. He, C. Zhang, X. Shi, B.-Q. He, J.-X. Wang, J. Environ. Sci. 16 (2004) 793.